

Helioseismic Fréchet Traveltime Kernels in Spherical Coordinates

R. B. Schlottmann and A. G. Kosovichev

W. W. Hansen Experimental Physics Laboratory, Stanford University

Stanford, CA 94305

briansch@fusemail.com

Received _____; accepted _____

To be submitted to *The Astrophysical Journal*

arXiv:1105.4619v2 [astro-ph.SR] 20 Jun 2011

ABSTRACT

Seismic traveltimes measurements are a crucial tool in the investigation of the solar interior, particularly in the examination of fine-scale structure. Traditional analysis of traveltimes relies on a geometrical ray picture of acoustic wave propagation, which assumes high frequencies. However, it is well-known that traveltimes obtained from finite-frequency waves are sensitive to variations of medium parameters in a wide Fresnel zone around the ray path. To address this problem, Fréchet traveltimes sensitivity kernels have previously been developed. These kernels use a more realistic approximation of the wave propagation to obtain a linear relationship between traveltimes and variations in medium parameters. Fréchet kernels take into account the actual frequency content of the measured waves and, thus, reproduce the Fresnel zone. Kernel theory has been well-developed in previous work on plane-parallel models of the Sun for use in local helioseismology. Our primary purpose is to apply kernel theory to much larger scales and in a spherical geometry. We also present kernel theory in a different way, using basic functional analytic methods, in the hope that this approach provides an even clearer understanding of the theory, as well as a set of tools for calculating kernels. Our results are very general and can be used to develop kernels for sensitivity to sound speed, density, magnetic fields, fluid flows, and any other medium parameter which can affect wave propagation.

1. INTRODUCTION

In both the Sun and the Earth, the passage of waves, acoustic or elastic, respectively, through the body yields an indispensable probe of the inner structure and physics that

would otherwise be unavailable. Both helioseismology and geoseismology have relied on the inversion of normal mode data and time-distance measurements to obtain information on their subjects’ interiors. In both fields, the time-distance measurements are the data that are more sensitive to small-scale, three-dimensional variations in structural parameters such as wave speed and density.

Traditionally, the measurements of traveltimes have been interpreted using a geometrical ray approximation to the wave propagation. However, it has long been appreciated that this approximation is generally inadequate, geometrical rays being accurate representations of waves only at very small wavelengths relative to variations in medium parameters. In reality, the arrival time of a wave packet associated with a particular ray path is sensitive to structure well off the ray, the width of that “Fresnel zone” being dependent on the dominant frequencies in the wave.

In an effort to obtain better information on the Earth’s interior, geoseismologists developed traveltime sensitivity kernels (See, e.g., Dahlen et al. 2000; Hung et al. 2000), which account for the finite frequency nature of the waves. By more accurately representing the physics of wave propagation, these kernels provide a better “map” between structure and traveltimes, which, in turn, yields a more accurate inversion result.

Traveltime kernels are not new to helioseismology. Gizon & Birch (2002) developed 2D kernels for f-mode traveltime sensitivity to acoustic damping and excitation, while Birch et al. (2004), using a plane-parallel model of the Sun’s near-surface, developed 3D traveltime kernels for perturbations in sound speed and density. In both papers the theoretical foundations of sensitivity kernels, as well as practical considerations in their calculation, were laid out clearly and accurately. We will rely most heavily on those two sources to guide us in this work.

The primary purpose of this paper is to further generalize the work of Gizon & Birch

(2002) and Birch et al. (2004) to a spherical geometry, which would allow the development of kernels for deep Sun structure, an area of active interest (Zhao et al. 2009) . However, we also wish to present the theory using the tools of basic functional analysis, with the hope that this way of looking at kernels provides an even clearer understanding of their nature.

Our theoretical results are quite general and can be used to develop kernels for various structural parameters. Not only can formulas for sensitivity to sound speed and density be obtained, but one can also derive kernels for magnetic fields, fluid flows, and damping. In principle, the sensitivity to any parameter which can affect the propagation of waves can be derived.

2. INTRODUCTION TO KERNEL THEORY

In this section, we lay out a fairly general development of helioseismic traveltime sensitivity kernels based on the Born approximation. In geoseismology, where their theory and application were first developed, they are frequently called Fréchet kernels or, more colorfully, “banana-doughnut” kernels, because of their characteristic appearance in cross-section. As will be made precise later, these kernels quantify the first-order (i.e., linear) dependence of seismic traveltimes on perturbations of any physical properties of a medium that can affect the propagation of seismic waves. By perturbation, we mean the difference between the value of a property for a particular medium and that of a reference medium. Usually, the reference medium is taken to be one with a high degree of symmetry, which greatly reduces the computational cost of calculating kernels. In the case of both the Sun and the Earth, this means that the reference model is most often spherically symmetric.

The theoretical results contained in this section are not particularly novel. Kernels have been developed previously for the Sun in Cartesian coordinates and for the Earth (which

has somewhat different wave propagation effects from the Sun) in spherical coordinates. However, the development presented here utilizes a different theoretical apparatus which may be clearer and cleaner in some ways than the usual derivations. In particular, heavy use is made of some basic concepts in functional analysis. These concepts are not complicated, but since they may not be familiar to every reader, we give below a non-rigorous review of what will be needed. (See Hatfield 1992, ch. 9, for a nice review of functional calculus.)

2.1. Basic Functional Analysis

First, we define a functional as a “function over function space” or, more precisely, a mapping from a space of functions to a finite-dimensional space of real or complex numbers. If f is a functional of a function g and itself a *function* of a variable x , we denote this as $f[g](x)$. A relevant example would be the acoustic displacement wavefield, \mathbf{u} , in a medium of sound speed c . Since the field is a function of position and time as well as a functional over the space of sound speed models, we would denote it here by $\mathbf{u}[c](\mathbf{x}, t)$.

The workhorse in our use of functional analysis will be the functional derivative, which is formally (i.e., non-rigorously) defined as

$$\frac{\delta f[g]}{\delta g(a)} = \lim_{\varepsilon \rightarrow 0} \frac{f[g(\cdot) + \varepsilon \delta(\cdot - a)] - f[g(\cdot)]}{\varepsilon}, \quad (1)$$

where the dot in $g(\cdot)$, for example, is a placeholder for the unspecified argument of function g . It may be useful to conceptualize the functional derivative as a gradient in an infinite dimensional space, with the value of the function at each point in physical space viewed as one coordinate of the function’s “position” in function space.

One consequence of our definition is that if

$$f[g](x) = \int_{-\infty}^{\infty} dx' g(x') \delta(x - x') = g(x), \quad (2)$$

then our definition of the functional derivative implies

$$\frac{\delta f[g](x)}{\delta g(a)} = \frac{\delta g(x)}{\delta g(a)} = \delta(x - a), \quad (3)$$

which is a result we will use often.

The only other concept from functional analysis we need is that of the functional Taylor series. If f is a functional over some function space, then f can be expanded about some specific function g_0 :

$$f[g] = f[g_0] + \int_{-\infty}^{\infty} dx' \Delta g(x') \left. \frac{\delta f[g]}{\delta g(x')} \right|_{g_0} + \frac{1}{2!} \int_{-\infty}^{\infty} dx'' \int_{-\infty}^{\infty} dx' \Delta g(x') \Delta g(x'') \left. \frac{\delta^2 f[g]}{\delta g(x'') \delta g(x')} \right|_{g_0} + \dots \quad (4)$$

where

$$\Delta g(\cdot) = g(\cdot) - g_0(\cdot). \quad (5)$$

Note that all the above concepts relationships extend in an obvious way to functionals over functions of several variables as well as to functionals over vector functions.

2.2. Development of the Kernels

Here we define the inverse problem to be solved and present the mathematical derivation of the traveltimes kernels that arise from it. We first cover the definition of some basic observables, the precise definition of what we mean by “traveltimes”, and the linearization of the relationship between traveltimes and actual medium properties. We then connect the results explicitly to wavefields in a reference solar model, providing general formulas for the kernels in terms of observational constraints (such as filters, line-of-sight effects, etc.), the reference wavefields, and the differential operators that govern them.

2.2.1. Some Definitions and the Linearized Problem

Some care is required here in our definition of various quantities of interest since there are different observables which could be called the “wavefield” and different derived quantities which could be called the “data”. We will refer to the actual particle motion due to the propagation of helioseismic waves in the Sun as the “wavefield”. The measured line-of-sight dopplergrams will be called the “raw data” or “raw traces”, whereas the seismograms acquired by cross-correlating raw traces will be denoted “processed traces” or “processed data”.

In addition, we make a couple of brief comments about notation. To promote clarity, we indicate solar surface coordinates and integration variables by $\boldsymbol{\sigma}$, $\boldsymbol{\sigma}'$, and so forth, whereas interior coordinates and integration variables are denoted by \mathbf{x} and its variations. Also, unless otherwise stated, the Einstein summation convention is implied by repeated Latin indices.

We denote the particle velocity wavefield by $\mathbf{v}(\mathbf{x}, t)$ and the raw data by $\psi(\boldsymbol{\sigma}, t)$. These two are related by

$$\psi(\boldsymbol{\sigma}, t) = \int_{\partial\odot} d^2\boldsymbol{\sigma}' \int_{-\infty}^{\infty} dt' \mathbf{F}(\boldsymbol{\sigma}, \boldsymbol{\sigma}', t - t') \cdot \mathbf{v}(\boldsymbol{\sigma}', t') \quad (6)$$

where \mathbf{F} represents the action of all spatial and temporal filters, which are assumed to be linear and time-translation invariant, that result from the instrument response and from whatever other filters that may be applied later. Note that the direction of \mathbf{F} is along the line of sight from the point $\boldsymbol{\sigma}'$ to the instrument and that the integration is over the surface of the Sun.

The processed traces derived from the raw traces are denoted $D(\boldsymbol{\sigma}_a, \boldsymbol{\sigma}_b, t)$ and are obtained by cross-correlation of the raw traces associated with points $\boldsymbol{\sigma}_a$ and $\boldsymbol{\sigma}_b$ on the

solar surface:

$$D(\boldsymbol{\sigma}_a, \boldsymbol{\sigma}_b, t) = \int_{-\infty}^{\infty} dt' \psi(\boldsymbol{\sigma}_a, t + t') \psi(\boldsymbol{\sigma}_b, t'). \quad (7)$$

For simplicity, we will not account for the finite time length of raw traces but instead will approximate the cross-correlation as an integral over all time. Note that we have defined $D(\boldsymbol{\sigma}_a, \boldsymbol{\sigma}_b, t)$ in such a way that for positive times, the resulting seismograms represent waves travelling from $\boldsymbol{\sigma}_b$ to $\boldsymbol{\sigma}_a$.

We also define the quantities \mathbf{v}_0 , ψ_0 , and D_0 as the wavefield, raw data, and processed data, respectively, generated synthetically from a given reference solar model. Hereafter, any quantity with a subscript 0 is taken to be associated with the reference model.

We next define $C(\boldsymbol{\sigma}_a, \boldsymbol{\sigma}_b, t)$ as the windowed cross-correlation between the real and reference processed traces:

$$C(\boldsymbol{\sigma}_a, \boldsymbol{\sigma}_b, t) = \int_{-\infty}^{\infty} dt' W(\boldsymbol{\sigma}_a, \boldsymbol{\sigma}_b, t + t') D_0(\boldsymbol{\sigma}_a, \boldsymbol{\sigma}_b, t + t') W(\boldsymbol{\sigma}_a, \boldsymbol{\sigma}_b, t') D(\boldsymbol{\sigma}_a, \boldsymbol{\sigma}_b, t'). \quad (8)$$

The function W is a windowing function applied to both the real and reference data, the purpose of which is to isolate pulses associated with specific propagation paths.

Now let $\tau(\boldsymbol{\sigma}_a, \boldsymbol{\sigma}_b)$ be the time lag at which the cross-correlation above is maximum. We define this time as the traveltime. It is imperative to note that the traveltime *must* be measured this way before the kernels we derive here can be used. Other ways of measuring the traveltime are not necessarily better or worse, but they will require different kernels. We also point out that the way we have defined the cross-correlation ensures that if a pulse in the real data is early with respect to the reference data, then the traveltime will be *positive*. In other words, τ is a measure of how much the real pulse is advanced with respect to the reference.

The traveltime is a functional of the actual solar model. If we let \mathbf{q} and \mathbf{q}_0 denote vectors of functions describing the actual and reference solar models (e.g. $q_1(\mathbf{x})$ and $q_2(\mathbf{x})$)

could be, respectively, the sound speed and density as a function of space inside the real Sun), then we can expand τ in a functional Taylor series about \mathbf{q}_0 ,

$$\begin{aligned} \tau[\mathbf{q}](\boldsymbol{\sigma}_a, \boldsymbol{\sigma}_b) &= \tau[\mathbf{q}_0](\boldsymbol{\sigma}_a, \boldsymbol{\sigma}_b) + \sum_{\alpha} \int_{\odot} d^3\mathbf{x} \Delta q_{\alpha}(\mathbf{x}) \frac{\delta\tau}{\delta q_{\alpha}(\mathbf{x})}(\boldsymbol{\sigma}_a, \boldsymbol{\sigma}_b) \Big|_{\mathbf{q}_0} \\ &\quad + \frac{1}{2!} \sum_{\alpha, \beta} \int_{\odot} d^3\mathbf{x} \int_{\odot} d^3\mathbf{x}' \Delta q_{\alpha}(\mathbf{x}) \Delta q_{\beta}(\mathbf{x}') \frac{\delta^2\tau}{\partial q_{\beta}(\mathbf{x}') \partial q_{\alpha}(\mathbf{x})}(\boldsymbol{\sigma}_a, \boldsymbol{\sigma}_b) \Big|_{\mathbf{q}_0} + \dots, \end{aligned} \quad (9)$$

where $\Delta q_{\alpha}(\mathbf{x}) = q_{\alpha}(\mathbf{x}) - q_{0,\alpha}(\mathbf{x})$, and integration is over the volume of the Sun. The first term in the expansion is identically zero since the time lag between the real and reference data would be zero if the real model were the same as the reference. In order to get a linear inverse problem to be solved later, we need a linear relationship between the traveltime and the perturbations Δq_{α} to the solar model. This is accomplished by simply dropping the nonlinear terms in the above Taylor series. This is the *only* linearization required in this development of the kernels. Any other linearizations that occur later (e.g. the use of the first Born approximation) are a direct consequence of this one approximation and do not represent further approximations. However, this linearization does assume that the model perturbations are small in the sense that their main effect is to cause small changes in the arrival times of pulses in the real data. Larger perturbations invalidate this assumption because they can cause distortions in waveforms, not just time shifts, that make the cross-correlation traveltime measurements meaningless. Thus, hereafter we assume the equivalence

$$\tau(\boldsymbol{\sigma}_a, \boldsymbol{\sigma}_b) \equiv \sum_{\alpha} \int_{\odot} d^3\mathbf{x} \Delta q_{\alpha}(\mathbf{x}) \frac{\delta\tau}{\delta q_{\alpha}(\mathbf{x})}(\boldsymbol{\sigma}_a, \boldsymbol{\sigma}_b) \Big|_{\mathbf{q}_0}. \quad (10)$$

Traditionally, Fréchet kernels are defined in such a way that they provide a linear relationship between traveltimes and *fractional* perturbations in model parameters. Following this tradition, we define K_{α} , the kernel for the α -th model parameter, as

$$K_{\alpha}(\mathbf{x}; \boldsymbol{\sigma}_a, \boldsymbol{\sigma}_b) = q_{0,\alpha}(\mathbf{x}) \frac{\delta\tau}{\delta q_{\alpha}(\mathbf{x})}(\boldsymbol{\sigma}_a, \boldsymbol{\sigma}_b) \Big|_{\mathbf{q}_0}, \quad (11)$$

so that

$$\tau(\boldsymbol{\sigma}_a, \boldsymbol{\sigma}_b) \equiv \sum_{\alpha} \int_{\odot} d^3\mathbf{x} \frac{\Delta q_{\alpha}(\mathbf{x})}{q_{0,\alpha}(\mathbf{x})} K_{\alpha}(\mathbf{x}; \boldsymbol{\sigma}_a, \boldsymbol{\sigma}_b). \quad (12)$$

The remainder of this section will be devoted to relating the above expression, eq. (11), to calculable physical quantities and known observational constraints.

2.2.2. General Kernel Formulas

The expression in eq. (11) is useless until we connect it explicitly to the underlying physics governing helioseismic wave propagation. We begin by providing an explicit mathematical definition of τ . We have previously defined it as the value of the time lag that maximizes C , the windowed cross-correlation between the real and reference data. Letting $C(t) = C(\boldsymbol{\sigma}_a, \boldsymbol{\sigma}_b, t)$, we expand C in a Taylor series about $t = 0$:

$$C(t) = \sum_{n=0}^{\infty} \frac{t^n}{n!} C^{(n)}(0). \quad (13)$$

Making the reasonable assumption that C is a smooth function, we have that $C'(\tau) = 0$.

Thus,

$$C'(\tau) = \sum_{n=1}^{\infty} \frac{\tau^{n-1}}{(n-1)!} C^{(n)}(0) = 0. \quad (14)$$

Taking the first functional derivative of eq. (14) with respect to q_{α} at $\mathbf{q} = \mathbf{q}_0$, we get

$$0 = \left. \frac{\delta C'(\tau)}{\delta q_{\alpha}(\mathbf{x})} \right|_{\mathbf{q}_0} = \left. \frac{\delta C'(0)}{\delta q_{\alpha}(\mathbf{x})} \right|_{\mathbf{q}_0} + \sum_{n=2}^{\infty} \left[\frac{\tau^{n-2}}{(n-2)!} C^{(n)}(0) \frac{\delta \tau}{\delta q_{\alpha}(\mathbf{x})} + \frac{\tau^{n-1}}{(n-1)!} \frac{\delta C^{(n)}(0)}{\delta q_{\alpha}(\mathbf{x})} \right] \Big|_{\mathbf{q}_0}. \quad (15)$$

Since $\tau[\mathbf{q}_0] = 0$, the above reduces to

$$0 = \left. \frac{\delta C'(0)}{\delta q_{\alpha}(\mathbf{x})} \right|_{\mathbf{q}_0} + C_0''(0) \left. \frac{\delta \tau}{\delta q_{\alpha}(\mathbf{x})} \right|_{\mathbf{q}_0}, \quad (16)$$

which implies

$$\left. \frac{\delta \tau}{\delta q_{\alpha}(\mathbf{x})} \right|_{\mathbf{q}_0} = -\frac{1}{C_0''(0)} \left. \frac{\delta C'(0)}{\delta q_{\alpha}(\mathbf{x})} \right|_{\mathbf{q}_0}, \quad (17)$$

where

$$C_0(t) = \int_{-\infty}^{\infty} dt' W(\boldsymbol{\sigma}_a, \boldsymbol{\sigma}_b, t+t') D_0(\boldsymbol{\sigma}_a, \boldsymbol{\sigma}_b, t+t') W(\boldsymbol{\sigma}_a, \boldsymbol{\sigma}_b, t') D_0(\boldsymbol{\sigma}_a, \boldsymbol{\sigma}_b, t'). \quad (18)$$

Eq. (17) connects our definition of the kernel in eq. (11) to something readily related to actual wave propagation.

At this point, it will be more convenient to work in the frequency domain. To begin, we state our Fourier transform convention. If $f(t)$ is a function of time, then

$$\tilde{f}(\omega) = \frac{1}{\sqrt{2\pi}} \int_{-\infty}^{\infty} dt e^{i\omega t} f(t) \quad (19a)$$

$$f(t) = \frac{1}{\sqrt{2\pi}} \int_{-\infty}^{\infty} d\omega e^{-i\omega t} \tilde{f}(\omega). \quad (19b)$$

Now, if we define

$$U_n(\boldsymbol{\sigma}_a, \boldsymbol{\sigma}_b, t') \equiv \frac{d^n}{dt^n} \left[W(\boldsymbol{\sigma}_a, \boldsymbol{\sigma}_b, t+t') D_0(\boldsymbol{\sigma}_a, \boldsymbol{\sigma}_b, t+t') \right]_{t=0} W(\boldsymbol{\sigma}_a, \boldsymbol{\sigma}_b, t'), \quad (20)$$

where $n = 1, 2$, then from eq. (8)

$$C'(0) = \int_{-\infty}^{\infty} dt' U_1(\boldsymbol{\sigma}_a, \boldsymbol{\sigma}_b, t') D(\boldsymbol{\sigma}_a, \boldsymbol{\sigma}_b, t') \quad (21a)$$

$$= \int_{-\infty}^{\infty} d\omega \tilde{U}_1^*(\boldsymbol{\sigma}_a, \boldsymbol{\sigma}_b, \omega) \tilde{D}(\boldsymbol{\sigma}_a, \boldsymbol{\sigma}_b, \omega), \quad (21b)$$

and, similarly,

$$C_0''(0) = \int_{-\infty}^{\infty} d\omega \tilde{U}_2^*(\boldsymbol{\sigma}_a, \boldsymbol{\sigma}_b, \omega) \tilde{D}_0(\boldsymbol{\sigma}_a, \boldsymbol{\sigma}_b, \omega), \quad (22)$$

where we have used the fact that $U_{1,2}$ and D are real-valued. With eq. (21b) in hand, we find

$$\left. \frac{\delta C'(0)}{\delta q_\alpha(\mathbf{x})} \right|_{\mathbf{q}_0} = \int_{-\infty}^{\infty} d\omega \tilde{U}_1^*(\boldsymbol{\sigma}_a, \boldsymbol{\sigma}_b, \omega) \left. \frac{\delta \tilde{D}(\boldsymbol{\sigma}_a, \boldsymbol{\sigma}_b, \omega)}{\delta q_\alpha(\mathbf{x})} \right|_{\mathbf{q}_0}. \quad (23)$$

Thus, combining eqs. (11), (17), and (23), we have as an intermediate result

$$K_\alpha(\mathbf{x}; \boldsymbol{\sigma}_a, \boldsymbol{\sigma}_b) = -\frac{q_{0,\alpha}(\mathbf{x})}{C_0''(0)} \int_{-\infty}^{\infty} d\omega \tilde{U}_1^*(\boldsymbol{\sigma}_a, \boldsymbol{\sigma}_b, \omega) \left. \frac{\delta \tilde{D}(\boldsymbol{\sigma}_a, \boldsymbol{\sigma}_b, \omega)}{\delta q_\alpha(\mathbf{x})} \right|_{\mathbf{q}_0}. \quad (24)$$

Since we will deal only with linearized wave propagation, we know the wavefield obeys

$$\mathcal{L}\Upsilon(\mathbf{x}, \omega) = \tilde{\mathbf{S}}(\mathbf{x}, \omega) \quad (25)$$

where \mathcal{L} is some linear differential operator that depends on the model parameters \mathbf{q} , $\tilde{\mathbf{S}}$ is a source function, and Υ is a four-dimensional vector comprised of the particle displacement wavefield $\tilde{\mathbf{u}}$ and the pressure perturbation \tilde{P} . If $\tilde{\mathbf{G}}(\mathbf{x}, \omega; \mathbf{x}_0)$ is the Green's tensor in the actual solar model, i.e., if

$$\mathcal{L}\tilde{\mathbf{G}}(\mathbf{x}, \omega; \mathbf{x}_0) = \delta(\mathbf{x} - \mathbf{x}_0) \mathbf{I}, \quad (26)$$

where \mathbf{I} is the identity matrix, then the solution to eq. (25) can be written as

$$\Upsilon(\mathbf{x}, \omega) = \int_{\odot} d^3\mathbf{x}' \tilde{\mathbf{G}}(\mathbf{x}, \omega; \mathbf{x}') \cdot \tilde{\mathbf{S}}(\mathbf{x}', \omega). \quad (27)$$

With this, eq. (6) can be rewritten in the frequency domain as

$$\tilde{\psi}(\boldsymbol{\sigma}, \omega) = \sqrt{2\pi} \int_{\partial\odot} d^2\boldsymbol{\sigma}' \int_{\odot} d^3\mathbf{x}' \tilde{F}_i(\boldsymbol{\sigma}, \boldsymbol{\sigma}', \omega) \tilde{G}_{ij}(\boldsymbol{\sigma}', \omega; \mathbf{x}') \tilde{S}_j(\mathbf{x}', \omega), \quad (28)$$

where we take $\tilde{\mathbf{F}}$ to have zero pressure component. Using this in the definition of D , eq. (7), we get

$$\begin{aligned} \tilde{D}(\boldsymbol{\sigma}_a, \boldsymbol{\sigma}_b, \omega) &= \sqrt{2\pi} \tilde{\psi}(\boldsymbol{\sigma}_a, \omega) \tilde{\psi}^*(\boldsymbol{\sigma}_b, \omega) \\ &= \int_{\partial\odot} d^2\boldsymbol{\sigma}_1 \int_{\odot} d^3\mathbf{x}_1 \int_{\partial\odot} d^2\boldsymbol{\sigma}_2 \int_{\odot} d^3\mathbf{x}_2 \tilde{F}_i(\boldsymbol{\sigma}_a, \boldsymbol{\sigma}_1, \omega) \tilde{G}_{ij}(\boldsymbol{\sigma}_1, \omega; \mathbf{x}_1) \tilde{S}_j(\mathbf{x}_1, \omega) \\ &\quad \times \tilde{F}_k^*(\boldsymbol{\sigma}_b, \boldsymbol{\sigma}_2, \omega) \tilde{G}_{kl}^*(\boldsymbol{\sigma}_2, \omega; \mathbf{x}_2) \tilde{S}_l^*(\mathbf{x}_2, \omega). \end{aligned} \quad (29)$$

Regarding the source terms appearing above, we note that it is understood that the acoustic excitation in the Sun is due to turbulent convection just below the photosphere and are often modeled stochastically. Following Birch et al. (2004), we choose to represent the excitation by a source covariance matrix, \mathbf{M} , defined as

$$M_{ij}(\mathbf{x}, \mathbf{x}', t) = \int_{-\infty}^{\infty} dt' S_i(\mathbf{x}, t + t') S_j(\mathbf{x}', t'), \quad (30)$$

or, in the frequency domain,

$$\tilde{M}_{ij}(\mathbf{x}, \mathbf{x}', \omega) = \tilde{S}_i(\mathbf{x}, \omega) \tilde{S}_j^*(\mathbf{x}', \omega). \quad (31)$$

(The value of using this representation will come later when we use a fairly simple reference model of the ensemble average of $\tilde{\mathbf{M}}$. However, we will also consider the possibility that the true form of $\tilde{\mathbf{M}}$ could be taken as one of the model parameters in \mathbf{q} .) Using this definition, eq. (29) becomes

$$\begin{aligned} \tilde{D}(\boldsymbol{\sigma}_a, \boldsymbol{\sigma}_b, \omega) &= \int_{\partial\odot} d^2\boldsymbol{\sigma}_1 \int_{\odot} d^3\mathbf{x}_1 \int_{\partial\odot} d^2\boldsymbol{\sigma}_2 \int_{\odot} d^3\mathbf{x}_2 \tilde{F}_i(\boldsymbol{\sigma}_a, \boldsymbol{\sigma}_1, \omega) \tilde{G}_{ij}(\boldsymbol{\sigma}_1, \omega; \mathbf{x}_1) \\ &\quad \times \tilde{F}_k^*(\boldsymbol{\sigma}_b, \boldsymbol{\sigma}_2, \omega) \tilde{G}_{kl}^*(\boldsymbol{\sigma}_2, \omega; \mathbf{x}_2) \tilde{M}_{jl}(\mathbf{x}_1, \mathbf{x}_2, \omega) \end{aligned} \quad (32)$$

Within eq. (32), only the Green's functions and the source covariance matrix are ever dependent on the model parameters. Thus, for simplicity, when we take the functional derivative of \tilde{D} , we separate those out and define the quantity

$$\tilde{R}_{\alpha, ik}(\mathbf{x}; \boldsymbol{\sigma}_1, \boldsymbol{\sigma}_2, \omega) = \frac{\delta}{\delta q_\alpha(\mathbf{x})} \int_{\odot} d^3\mathbf{x}_1 \int_{\odot} d^3\mathbf{x}_2 \tilde{G}_{ij}(\boldsymbol{\sigma}_1, \omega; \mathbf{x}_1) \tilde{G}_{kl}^*(\boldsymbol{\sigma}_2, \omega; \mathbf{x}_2) \tilde{M}_{jl}(\mathbf{x}_1, \mathbf{x}_2, \omega) \Big|_{\mathbf{q}_0}. \quad (33)$$

In order to evaluate this, we will need the functional derivative of \mathbf{G} . We start by taking the derivative of both sides of eq. (26), bearing in mind that the right hand side does not depend on the model parameters,

$$\frac{\delta \mathcal{L}}{\delta q_\alpha(\mathbf{x})} \Big|_{\mathbf{q}_0} \tilde{\mathbf{G}}_0(\mathbf{x}', \omega; \mathbf{x}_0) + \mathcal{L}_0 \frac{\delta \tilde{\mathbf{G}}(\mathbf{x}', \omega; \mathbf{x}_0)}{\delta q_\alpha(\mathbf{x})} \Big|_{\mathbf{q}_0} = 0, \quad (34)$$

where \mathcal{L}_0 and $\tilde{\mathbf{G}}_0$ are the wave equation differential operator and Green's function, respectively, for the reference model. The solution to this equation is

$$\frac{\delta \tilde{\mathbf{G}}(\mathbf{x}', \omega; \mathbf{x}_0)}{\delta q_\alpha(\mathbf{x})} \Big|_{\mathbf{q}_0} = - \int_{\odot} d^3\mathbf{x}'' \tilde{\mathbf{G}}_0(\mathbf{x}', \omega; \mathbf{x}'') \cdot \left[\frac{\delta \mathcal{L}(\mathbf{x}'', \omega)}{\delta q_\alpha(\mathbf{x})} \Big|_{\mathbf{q}_0} \tilde{\mathbf{G}}_0(\mathbf{x}'', \omega; \mathbf{x}_0) \right]. \quad (35)$$

Putting all of our results together so far, we quote our general equations for the desired Fréchet traveltime kernels:

$$K_\alpha(\mathbf{x}; \boldsymbol{\sigma}_a, \boldsymbol{\sigma}_b) = \frac{-q_{0,\alpha}(\mathbf{x})}{C_0''(\boldsymbol{\sigma}_a, \boldsymbol{\sigma}_b, 0)} \int_{-\infty}^{\infty} d\omega \int_{\partial\odot} d^2\boldsymbol{\sigma}_1 \int_{\partial\odot} d^2\boldsymbol{\sigma}_2 \tilde{U}_1^*(\boldsymbol{\sigma}_a, \boldsymbol{\sigma}_b, \omega) \tilde{F}_i(\boldsymbol{\sigma}_a, \boldsymbol{\sigma}_1, \omega) \tilde{F}_k^*(\boldsymbol{\sigma}_b, \boldsymbol{\sigma}_2, \omega) \times \tilde{R}_{\alpha,ik}(\mathbf{x}; \boldsymbol{\sigma}_1, \boldsymbol{\sigma}_2, \omega) \quad (36)$$

where

$$\begin{aligned} \tilde{R}_{\alpha,ik}(\mathbf{x}; \boldsymbol{\sigma}_1, \boldsymbol{\sigma}_2, \omega) = & \int_{\odot} d^3\mathbf{x}_1 \int_{\odot} d^3\mathbf{x}_2 \left\{ \tilde{G}_{0,ij}(\boldsymbol{\sigma}_1, \omega; \mathbf{x}_1) \tilde{G}_{0,kl}^*(\boldsymbol{\sigma}_2, \omega; \mathbf{x}_2) \frac{\delta \tilde{M}_{jl}(\mathbf{x}_1, \mathbf{x}_2, \omega)}{\delta q_\alpha(\mathbf{x})} \Big|_{\mathbf{q}_0} \right. \\ & - \int_{\odot} d^3\mathbf{x}'' \left[\tilde{G}_{0,im}(\boldsymbol{\sigma}_1, \omega; \mathbf{x}'') \left(\frac{\delta \mathcal{L}(\mathbf{x}'', \omega)}{\delta q_\alpha(\mathbf{x})} \Big|_{\mathbf{q}_0} \tilde{\mathbf{G}}_0(\mathbf{x}'', \omega; \mathbf{x}_1) \right)_{mj} \tilde{G}_{0,kl}^*(\boldsymbol{\sigma}_2, \omega; \mathbf{x}_2) \right. \\ & \left. \left. + \tilde{G}_{0,ij}(\boldsymbol{\sigma}_1, \omega; \mathbf{x}_1) \tilde{G}_{0,kn}^*(\boldsymbol{\sigma}_2, \omega; \mathbf{x}'') \left(\frac{\delta \mathcal{L}(\mathbf{x}'', \omega)}{\delta q_\alpha(\mathbf{x})} \Big|_{\mathbf{q}_0} \tilde{\mathbf{G}}_0(\mathbf{x}'', \omega; \mathbf{x}_2) \right)_{nl}^* \right] \tilde{M}_{0,jl}(\mathbf{x}_1, \mathbf{x}_2, \omega) \right\}. \quad (37) \end{aligned}$$

We note that the presence of three coupled volumetric integrals in eq. (37) would seem to make the calculation of the raw kernel computationally impractical. However, the functional derivatives of the linear wave operator generally will be proportional to three-dimensional spatial delta functions and their derivatives. Additionally, the reference source covariance matrix can be taken to be proportional to delta functions. Thus, the actual computational burden is much smaller than one might fear from the above result. We will see this in specific examples for kernels, such as those for sound speed and density.

3. SOME SPECIFIC KERNEL FORMULAS

In this section, we specify the aspects of acoustic wave propagation that we will consider and apply our general kernel formulas to a particular reference model of the Sun's structure and ensemble average of the source covariance matrix. We then give formulas for sensitivity kernels for perturbations in sound speed squared and density.

3.1. The Wave Equation and Reference Model

In order to use the kernel formulas we have developed, we must make assumptions about the physics of acoustic wave propagation both in the Sun and in our reference model. Only then can we calculate our reference Green’s functions and the functional derivatives of the wave equation operator that are needed.

From here on, we will assume that there are no magnetic fields or bulk fluid flows present in the Sun. Additionally, we will work in the Cowling approximation, i.e., we assume that the density variations induced by the propagation of an acoustic wave have a negligible effect on the gravitational potential. For all but the lowest degree modes, this approximation is extremely accurate. In future work, we will relax most if not all of these restrictions.

We will also include damping in our wave equation. For simplicity, we will somewhat follow Birch et al. (2004) and use a simple convolutional model in the time domain. However, in contrast to their work, we will assume that the attenuation operator is spatially local.

As for boundary conditions, we again follow Birch et al. (2004) and use a free surface boundary condition, i.e., we set the Lagrangian pressure equal to zero at some radius. As noted in Birch et al. (2004), this does, of course, mean that waves with frequencies above the acoustic cutoff do not escape the Sun but are reflected back into it, in disagreement with reality.

Under the above assumptions, the linearized equations for particle displacement $\tilde{\mathbf{u}}$ and

pressure perturbation \tilde{P}' have the following well-known form in the frequency domain:

$$-\omega^2 \rho \tilde{\mathbf{u}} + \nabla \tilde{P}' - \mathbf{g} \left[\frac{\tilde{P}'}{c^2} + \frac{\rho}{c^2} \mathbf{g} \cdot \tilde{\mathbf{u}} - (\nabla \rho) \cdot \tilde{\mathbf{u}} \right] - i\omega \rho \Gamma \tilde{\mathbf{u}} = 0, \quad (38)$$

$$\tilde{P}' + c^2 \rho \nabla \cdot \tilde{\mathbf{u}} + \rho \mathbf{g} \cdot \tilde{\mathbf{u}} = 0, \quad (39)$$

where c and ρ are the sound speed and density, respectively, \mathbf{g} is the gravitational acceleration, ω is the angular frequency, and Γ is the damping parameter. For the real Sun, we assume that all of the medium parameters above can vary spatially in all three dimensions but not in time. In the case of the damping parameter, we assume that it also varies in frequency so that in the time domain it is convolved with the particle velocity \mathbf{v} .

However, for the purpose of constructing our wave equation operator \mathcal{L} , we will rewrite eq. (39) slightly:

$$-\frac{1}{\rho c^2} \tilde{P}' - \nabla \cdot \tilde{\mathbf{u}} - \frac{\mathbf{g}}{c^2} \cdot \tilde{\mathbf{u}} = 0. \quad (40)$$

With this modification, our wave equation, eq. (25), becomes

$$\mathcal{L} \begin{bmatrix} \tilde{\mathbf{u}} \\ \tilde{P}' \end{bmatrix} = \begin{bmatrix} -(\omega^2 + i\omega\Gamma)\rho\mathbf{I} - \frac{\rho}{c^2} \mathbf{g}\mathbf{g}^{\mathbf{T}} + \mathbf{g}(\nabla\rho)^{\mathbf{T}} & \nabla - \frac{\mathbf{g}}{c^2} \\ -\nabla^{\mathbf{T}} - \frac{\mathbf{g}^{\mathbf{T}}}{c^2} & -\frac{1}{\rho c^2} \end{bmatrix} \begin{bmatrix} \tilde{\mathbf{u}} \\ \tilde{P}' \end{bmatrix} = \tilde{\mathbf{S}}, \quad (41)$$

where all vector quantities (and ∇) are taken to be column vectors and \mathbf{T} indicates transposition. The reason for using eq. (40) is that in this form, the Green's matrix corresponding to \mathcal{L} satisfies reciprocity, i.e.,

$$\tilde{\mathbf{G}}(\mathbf{x}, \omega; \mathbf{x}_0) = \tilde{\mathbf{G}}^{\mathbf{T}}(\mathbf{x}_0, \omega; \mathbf{x}), \quad (42)$$

Having a Green's matrix that obeys reciprocity greatly reduces the computational cost of computing kernels by limiting the number of source points for which we need to calculate responses, at least when one uses a technique other than mode summation, as we do.

With a specific form of \mathcal{L} now given, we are in position to calculate its functional derivatives. In this paper, we will concern ourselves with kernels for sound speed squared

and density, so we only need the functional derivatives with respect to those quantities:

$$\left. \frac{\delta \mathcal{L}(\mathbf{x})}{\delta c^2(\mathbf{x}')}\right|_{\mathbf{q}_0} = \frac{1}{c_0^4} \delta(\mathbf{x} - \mathbf{x}') \begin{bmatrix} \rho_0 \mathbf{g}_0 \mathbf{g}_0^T & \mathbf{g}_0 \\ \mathbf{g}_0^T & \frac{1}{\rho_0} \end{bmatrix}, \quad (43)$$

$$\left. \frac{\delta \mathcal{L}(\mathbf{x})}{\delta \rho(\mathbf{x}')}\right|_{\mathbf{q}_0} = \delta(\mathbf{x} - \mathbf{x}') \begin{bmatrix} -(\omega^2 + i\omega\Gamma_0)\mathbf{I} - \frac{1}{c_0^2} \mathbf{g}_0 \mathbf{g}_0^T & 0 \\ 0 & \frac{1}{\rho_0^2 c_0^2} \end{bmatrix} + \begin{bmatrix} \mathbf{g}_0 \nabla^T \delta(\mathbf{x} - \mathbf{x}') & 0 \\ 0 & 0 \end{bmatrix}. \quad (44)$$

In eq. (44) we have neglected the derivative of \mathbf{g} with respect to density under the assumption that the deviations in density from our reference model will cause such small changes in gravity that they will have a negligible effect on wave propagation. Note that this assumption is separate from the Cowling approximation.

In addition to laying out our assumptions about wave propagation in the Sun, we must also describe our reference model. The obvious choice for a model of the Sun's structure is one that is spherically symmetric and in hydrostatic equilibrium. The symmetry of this choice greatly simplifies the calculation of the Green's functions we will need.

As for the reference model of acoustic excitation, we will assume a simple form for the ensemble average of the source covariance matrix, eq. (31). We choose to generalize Birch et al. (2004) model to spherical coordinates:

$$\langle \tilde{M}_{ij}(\mathbf{x}, \mathbf{x}', \omega) \rangle = \delta_{ir} \delta_{jr} \frac{\delta(\theta - \theta') \delta(\phi - \phi')}{r^2 r'^2 \sin \theta} \delta'(r - r_s) \delta'(r' - r_s) |\tilde{f}(\omega)|^2, \quad (45)$$

where a subscript r indicates a component in the radial direction, and $|\tilde{f}(\omega)|^2$ is the power spectrum of the excitation and may be adjusted to ensure that the waves modelled in the reference medium have an acoustic power spectrum close to the Sun's. Note that this a very practical model of excitation, not necessarily a realistic one. In particular, the presence of the δ -functions in the angular variables, which implies a zero horizontal correlation length

for the sources, simplifies the computational effort required to model the excitation. As noted in Gizon & Birch (2002), the true correlation length of the sources is much smaller than the wavelengths of the waves we will model, anyway.

3.2. Kernel Formulas for Perturbations to c^2 and ρ

With our above assumptions in hand, we can now construct our sound speed and density kernel formulas. To begin, we introduce some simplifying notation. Recalling that our Green's function is a 4×4 matrix corresponding to a coupled system of equations in both particle displacement and pressure perturbation, we indicate its components by the indices r , θ , ϕ , and p , denoting the three directions in spherical coordinates and pressure. For instance, $G_{0,rp}(\mathbf{x}, \omega; \mathbf{x}_0)$ denotes the radial component of displacement at point \mathbf{x} due to a point pressure source at \mathbf{x}_0 , in the reference medium, at frequency ω . When we wish to leave a component unspecified (or indicate Einstein summation), we use Latin indices (other than r or p).

To construct our kernel formulas, we start by incorporating the source excitation model, eq. (45), into eq. (37), which we write as

$$\tilde{R}_{\alpha,ik}(\mathbf{x}; \boldsymbol{\sigma}_1, \boldsymbol{\sigma}_2, \omega) = H_{\alpha,ik}(\mathbf{x}; \boldsymbol{\sigma}_1, \boldsymbol{\sigma}_2, \omega) + H_{\alpha,ki}^*(\mathbf{x}; \boldsymbol{\sigma}_2, \boldsymbol{\sigma}_1, \omega) \quad (46)$$

where

$$H_{\alpha,ik}(\mathbf{x}; \boldsymbol{\sigma}_1, \boldsymbol{\sigma}_2, \omega) = - \int_{\partial\odot} d^2\boldsymbol{\sigma}' \int_{\odot} d^3\mathbf{x}'' \tilde{G}_{0,im}(\boldsymbol{\sigma}_1, \omega; \mathbf{x}'') \left(\frac{\delta\mathcal{L}(\mathbf{x}'', \omega)}{\delta q_\alpha(\mathbf{x})} \Big|_{\mathbf{q}_0} \partial_{r_s} \tilde{\mathbf{G}}_0(\mathbf{x}'', \omega; r_s, \boldsymbol{\sigma}') \right)_{mr} \partial_{r_s} \tilde{G}_{0,kr}^*(\boldsymbol{\sigma}_2, \omega; r_s, \boldsymbol{\sigma}') \quad (47)$$

Note that ∂_{r_s} is shorthand for partial differentiation with respect to r_s , and we have assumed that the source covariance is fixed.

Now using eqs. (43) and (44) and recognizing that $\mathbf{g}_0 = -g_0 \hat{r}$, we get

$$\begin{aligned}
 H_{c^2}(\mathbf{x}; \boldsymbol{\sigma}_1, \boldsymbol{\sigma}_2, \omega) = & \\
 & - \frac{1}{c_0^4} \int_{\partial\odot} d^2\boldsymbol{\sigma}' \left[\tilde{G}_{0,rr}(\boldsymbol{\sigma}_1, \omega; \mathbf{x}) \left(\rho_0 g_0^2 \partial_{r_s} \tilde{G}_{0,rr}(\mathbf{x}, \omega; r_s, \boldsymbol{\sigma}') - g_0 \partial_{r_s} \tilde{G}_{0,pr}(\mathbf{x}, \omega; r_s, \boldsymbol{\sigma}') \right) \right. \\
 & \left. + \tilde{G}_{0,rp}(\boldsymbol{\sigma}_1, \omega; \mathbf{x}) \left(-g_0 \partial_{r_s} \tilde{G}_{0,rr}(\mathbf{x}, \omega; r_s, \boldsymbol{\sigma}') + \frac{1}{\rho_0} \partial_{r_s} \tilde{G}_{0,pr}(\mathbf{x}, \omega; r_s, \boldsymbol{\sigma}') \right) \right] \\
 & \times \partial_{r_s} \tilde{G}_{0,rr}^*(\boldsymbol{\sigma}_2, \omega; r_s, \boldsymbol{\sigma}') \left| \tilde{f}(\omega) \right|^2 \quad (48)
 \end{aligned}$$

and

$$\begin{aligned}
 H_\rho(\mathbf{x}; \boldsymbol{\sigma}_1, \boldsymbol{\sigma}_2, \omega) = & - \int_{\partial\odot} d^2\boldsymbol{\sigma}' \left[-(\omega^2 + i\omega\Gamma) \sum_{m=r,\theta,\phi} \tilde{G}_{0,rm}(\boldsymbol{\sigma}_1, \omega; \mathbf{x}) \partial_{r_s} \tilde{G}_{0,mr}(\mathbf{x}, \omega; r_s, \boldsymbol{\sigma}') \right. \\
 & - \tilde{G}_{0,rr}(\boldsymbol{\sigma}_1, \omega; \mathbf{x}) \frac{g_0^2}{c_0^2} \partial_{r_s} \tilde{G}_{0,rr}(\mathbf{x}, \omega; r_s, \boldsymbol{\sigma}') + \tilde{G}_{0,rp}(\boldsymbol{\sigma}_1, \omega; \mathbf{x}) \frac{1}{\rho_0^2 c_0^2} \partial_{r_s} \tilde{G}_{0,pr}(\mathbf{x}, \omega; r_s, \boldsymbol{\sigma}') \\
 & + \partial_r \left(\tilde{G}_{0,rr}(\boldsymbol{\sigma}_1, \omega; \mathbf{x}) g_0 \partial_{r_s} \tilde{G}_{0,rr}(\mathbf{x}, \omega; r_s, \boldsymbol{\sigma}') \right) \\
 & + \frac{1}{r} \partial_\theta \left(\tilde{G}_{0,rr}(\boldsymbol{\sigma}_1, \omega; \mathbf{x}) g_0 \partial_{r_s} \tilde{G}_{0,\theta r}(\mathbf{x}, \omega; r_s, \boldsymbol{\sigma}') \right) \\
 & \left. + \frac{1}{r \sin \theta} \partial_\phi \left(\tilde{G}_{0,rr}(\boldsymbol{\sigma}_1, \omega; \mathbf{x}) g_0 \partial_{r_s} \tilde{G}_{0,\phi r}(\mathbf{x}, \omega; r_s, \boldsymbol{\sigma}') \right) \right] \\
 & \times \partial_{r_s} \tilde{G}_{0,rr}^*(\boldsymbol{\sigma}_2, \omega; r_s, \boldsymbol{\sigma}') \left| \tilde{f}(\omega) \right|^2, \quad (49)
 \end{aligned}$$

where all medium parameters are implicitly evaluated at \mathbf{x} .

Lastly, we need to incorporate our source covariance model into our formula for \tilde{D}_0 , the reference model version of eq. (29), which is needed in the evaluation of $U_{1,2}$ and C_0'' (eq. 22), which in turn are used in eq. (36). Using eq. (45), our formula for \tilde{D}_0 becomes

$$\begin{aligned}
 \tilde{D}_0(\boldsymbol{\sigma}_a, \boldsymbol{\sigma}_b, \omega) = & \int_{\partial\odot} d^2\boldsymbol{\sigma}_1 \int_{\partial\odot} d^2\boldsymbol{\sigma}_2 \int_{\partial\odot} d^2\boldsymbol{\sigma}', \tilde{F}_i(\boldsymbol{\sigma}_a, \boldsymbol{\sigma}_1, \omega) \partial_{r_s} \tilde{G}_{0,ir}(\boldsymbol{\sigma}_1, \omega; r_s, \boldsymbol{\sigma}') \\
 & \times \tilde{F}_k^*(\boldsymbol{\sigma}_b, \boldsymbol{\sigma}_2, \omega) \partial_{r_s} \tilde{G}_{0,kr}^*(\boldsymbol{\sigma}_2, \omega; r_s, \boldsymbol{\sigma}') \left| \tilde{f}(\omega) \right|^2. \quad (50)
 \end{aligned}$$

Thus, to construct traveltime sensitivity kernels for squared sound speed and density, under the assumptions laid out above, the equations that are needed are (20), (22), (36),

(46), and (48)-(50). Of course, the user of these results will still need to provide additional information, such as a specific reference model, observational geometry, and so forth.

4. EXAMPLES

In this section we display examples of kernels for squared sound speed for large distances, in order to give an idea of the extent and character of traveltime sensitivity at depth in the Sun. In order to accelerate the calculations somewhat, we make one particularly simplifying assumption, i.e., we take our filter function \mathbf{F} (see eq. 6) to be

$$\mathbf{F}(\boldsymbol{\sigma}, \boldsymbol{\sigma}', t) = \hat{r} \delta(\boldsymbol{\sigma} - \boldsymbol{\sigma}') \delta(t). \quad (51)$$

The assumption that the line of sight is always radial is quite helpful in lessening the computational complexity, but it is, of course, only a good approximation near the center of the Sun's visible disk.

As for our reference model, we use model S (Christensen-Dalsgaard et al. 1996) as the model of the Sun's structure, and a free-surface boundary condition, as mentioned earlier. For the power spectrum of the acoustic excitation, we once again turn to Birch et al. (2004) and use

$$\left| \tilde{f}(\omega) \right|^2 = e^{-\omega^2 T_{src}^2} \quad (52)$$

with $T_{src} = 68$ s.

Our damping model is actually a fusion of the ones used in Gizon & Birch (2002) and Birch et al. (2004). We let

$$\Gamma(\omega, r) = g(\omega)h(r), \quad (53)$$

where from Gizon & Birch (2002) we take

$$g(\omega) = \gamma \left| \frac{\omega}{\omega_*} \right|^\beta \quad (54)$$

with $\gamma/2\pi = 100\mu\text{Hz}$, $\omega_*/2\pi = 3\text{mHz}$, and $\beta = 4.4$. Whereas from Birch et al. (2004) we get

$$h(r) = \exp \left[-\frac{(T(r) - T_c)^2}{(\Delta t)^2} \right] \quad (55)$$

with

$$T(r) = \int_0^r \frac{dr'}{c_0(r')}, \quad (56)$$

$T_c = T(R)$, where R is the radius of the photosphere, and $\Delta t = 69$ s.

Lastly, we assume that our time window W is simply one for times within 10 m of a first arrival and zero otherwise.

In Fig. 1, we see our first example. Shown is a kernel for squared sound speed for two observation points separated by an angle of 30° . Because of the huge range of amplitudes in the kernel, the strongest regions being close to the observation points, we have scaled the kernel by the sound speed and saturated the scale in order to bring out the deep structure. Indicated in both cross-sections is the location of the ray path associated with the first arrival at this distance. Note that the kernel displays the classic “banana-doughnut” shape, with sensitivity reaching a local minimum on the ray path. The images here are limited to the upper 40% of the Sun, by radius. We can see that the kernel has sensitivity mostly in the convection zone and above.

In Fig. 2, we have the squared sound speed kernel for a distance of 60° . In this case, the sections show the upper 70% of the Sun. Clearly, the kernel in this case significantly intersects the tachocline, indicating that it may be of some use in interpreting time-distance measurements aimed at studying that region.

In both figures, it is clear that ray theory cannot be a good approximation here, given that the waves are clearly sensitive to a broad volume around the ray.

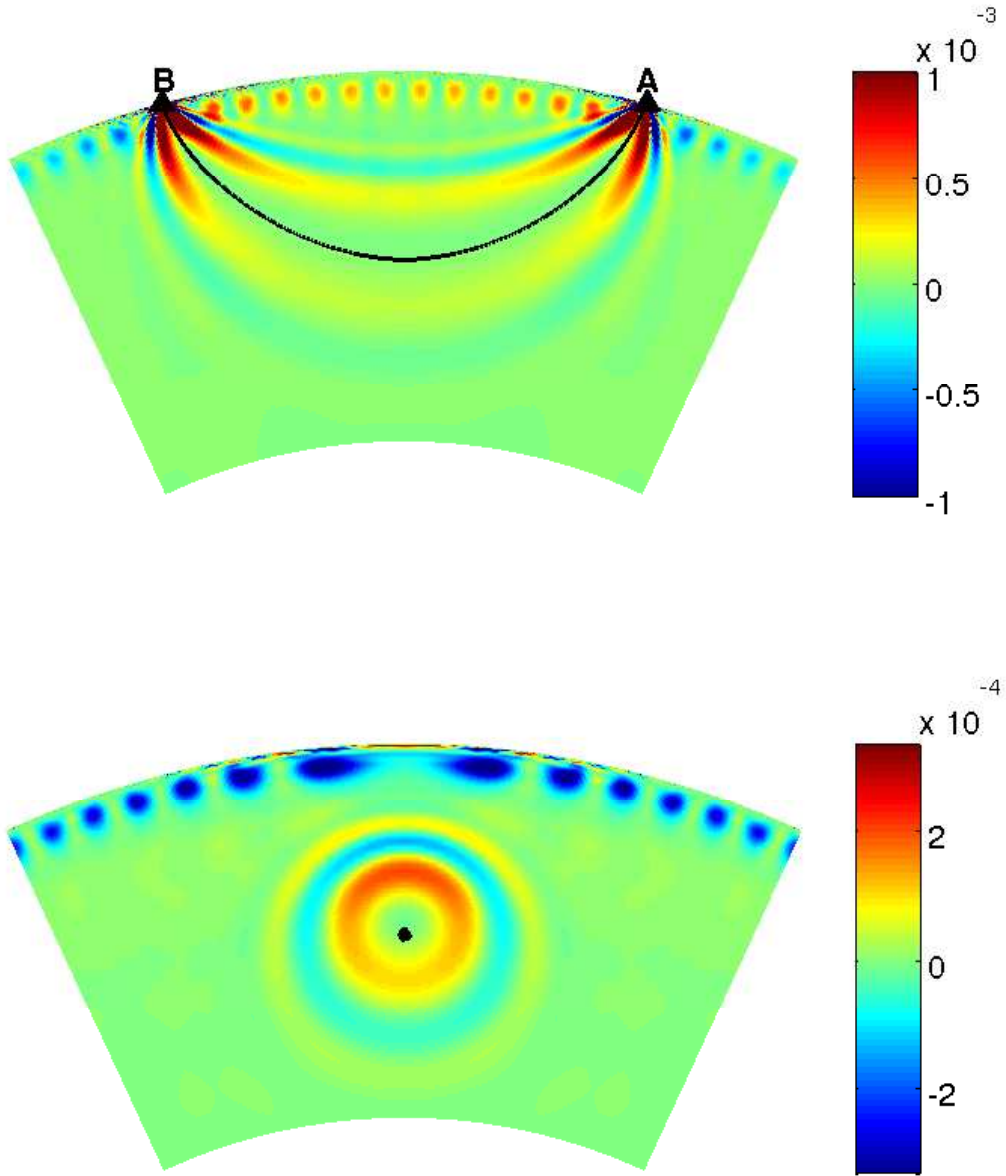


Fig. 1.— Vertical cross-sections of a sensitivity kernel for squared sound speed for a distance of 30° . The kernel has been scaled by the sound speed and the scale has been severely saturated. (*Top*) The cross-section in the plane of the ray path (black line). (*Bottom*) The cross-section perpendicular to the ray path. The intersection point of the plane and the ray is indicated by the black dot. The total angular range in both sections is 50° , and both extend radially from $0.6 R_\odot$ to the surface. Note that this is the kernel for waves travelling from point B to point A. The units are Mm^{-2}

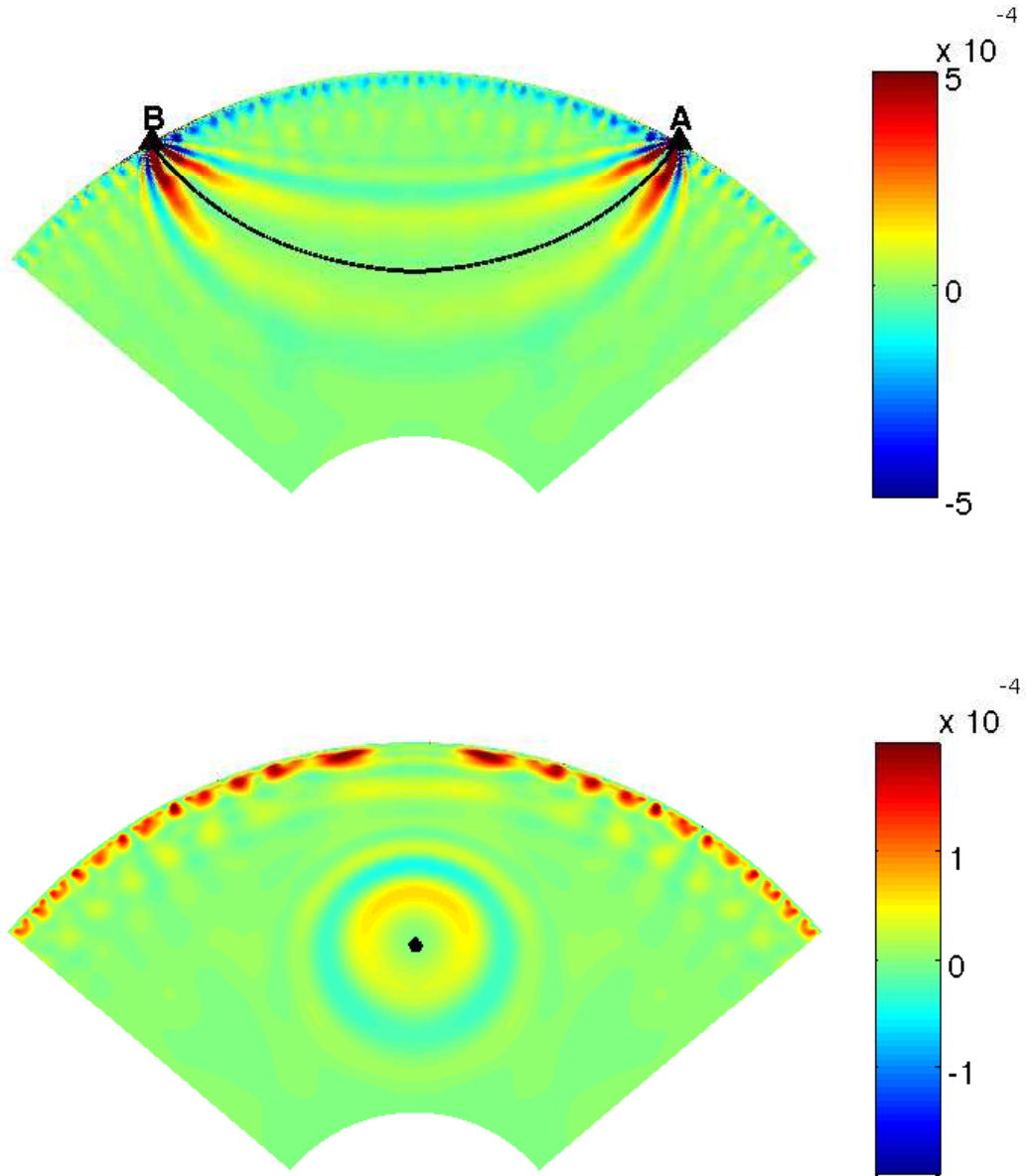


Fig. 2.— Vertical cross-sections of a sensitivity kernel for squared sound speed for a distance of 60° . Again the kernel has been scaled by the sound speed and the scale has been saturated. (*Top*) The cross-section in the plane of the ray path (black line). (*Bottom*) The cross-section perpendicular to the ray path. The intersection point of the plane and the ray is indicated by the black dot. The total angular range in both sections is 100° , and both extend radially from $0.3 R_\odot$ to the surface.

5. DISCUSSION

We have presented a different theoretical framework, based on functional analytic tools, that we hope many will find a clear and elegant way of thinking about traveltime sensitivity kernels. In addition, we have provided the essential formulas for calculating these kernels in a full spherical geometry. For kernels for medium properties other than the ones discussed here, the mathematical apparatus has been developed to allow the reader to derive his or her own formulas.

With some reasonable assumptions about the Sun, we have shown that one can obtain kernels that demonstrate their potential value by showing the inadequacy of ray theoretical approximations. Clearly these results can now be put to good use in analyzing time-distance measurements to obtain information on the deep structure of the Sun.

REFERENCES

Birch, A. C., Kosovichev, A. G., & Duvall, T. L., Jr., 2004, *ApJ*, 608, 580

Christensen-Dalsgaard, J., et al. 1996, *Science*, 272, 1286

Dahlen, F. A., Nolet, G., & Hung, S.-H. 2000, *Geophys. J. Int.*, 141, 157

Gizon, L., & Birch, A. C. 2002, *ApJ*, 571, 966

Hatfield, B. F. 1992, *Quantum Field Theory of Point Particles and Strings* (Redwood City: Addison-Wesley)

Hung, S.-H., Dahlen, F. A., & Nolet, G. 2000, *Geophys. J. Int.*, 141, 175

Zhao, J., Hartlep, T., Kosovichev, A. G., & Mansour, N. N. 2009, *ApJ*, 702, 1150